A MORPHOMETRIC STUDY ON THE THICKNESS OF THE PULMONARY AIR-BLOOD BARRIER

EWALD R. WEIBEL, M.D., and BRUCE W. KNIGHT

From The Rockefeller Institute. Dr. Weibel's present address is Anatomisches Institut der Universität, Zurich, Switzerland

ABSTRACT

A reliable knowledge of the thickness of the alveolo-capillary "membrane" or air-blood barrier is of physiologic interest since it is intimately related to a quantitative estimation of such functional events as gas diffusion or tissue metabolism in the lung. The characteristic thickness of the air-blood barrier with respect to gas diffusion is its harmonic mean thickness, while the arithmetic mean thickness is related to the mass of tissue building the barrier and consuming oxygen in the lung. Two morphometric methods are proposed by which these two dimensions can be estimated from random measurements in the electron microscope in a reliable, simple, and efficient manner. By applying these methods to three rat lungs the arithmetic mean thickness of the barrier was found to measure 1.25 μ, the harmonic mean thickness, 0.57 μ. On the basis of these measurements a geometric model of the barrier in the form of a corrugated membrane was derived. Its dimensions showed close similarity to those of the natural barrier. This analysis suggested furthermore that the gas conductance of the barrier is nearly optimal if one considers the mass of tissue and the minimal barrier thickness as fixed properties which are determined by other functional requirements on the alveolo-capillary membrane.

INTRODUCTION

At the level of alveoli and capillaries in the gas exchange region of the lung, air and blood are separated from each other by a thin sheet of tissue, the *alveolo-capillary* "membrane" or *air-blood barrier*. This membrane is essentially composed of a capillary endothelium and an alveolar epithelium which form continuous linings of capillaries and alveoli, respectively; these linings are separated, or joined, by a layer of interstitial tissue of varying composition and width (1–8).

The alveolo-capillary membrane is of physiological interest mainly in two respects. Firstly, it offers a certain resistance to gases diffusing between air and blood. The term "pulmonary diffusing capacity" of the physiologists implies, among other factors, the "membrane-diffusing capacity," which is a measure of the ease with which gases can cross the "membrane" (9–11). Secondly, this "membrane" is constructed of living tissues which metabolize oxygen at a critical place: the amount of oxygen metabolized is contained in the inspired air, but it is consumed before reaching the red blood cells in the alveolar capillaries and hence is not included in the oxygen measured in the arterial blood. This may cause difficulties in interpreting physiological data on gas exchange in the lung (12).

These functional implications are quantitatively determined by various structural properties of the alveolo-capillary membrane, particularly by its dimensions, extent and thickness, and by its composition. The extent of the "membrane" has been

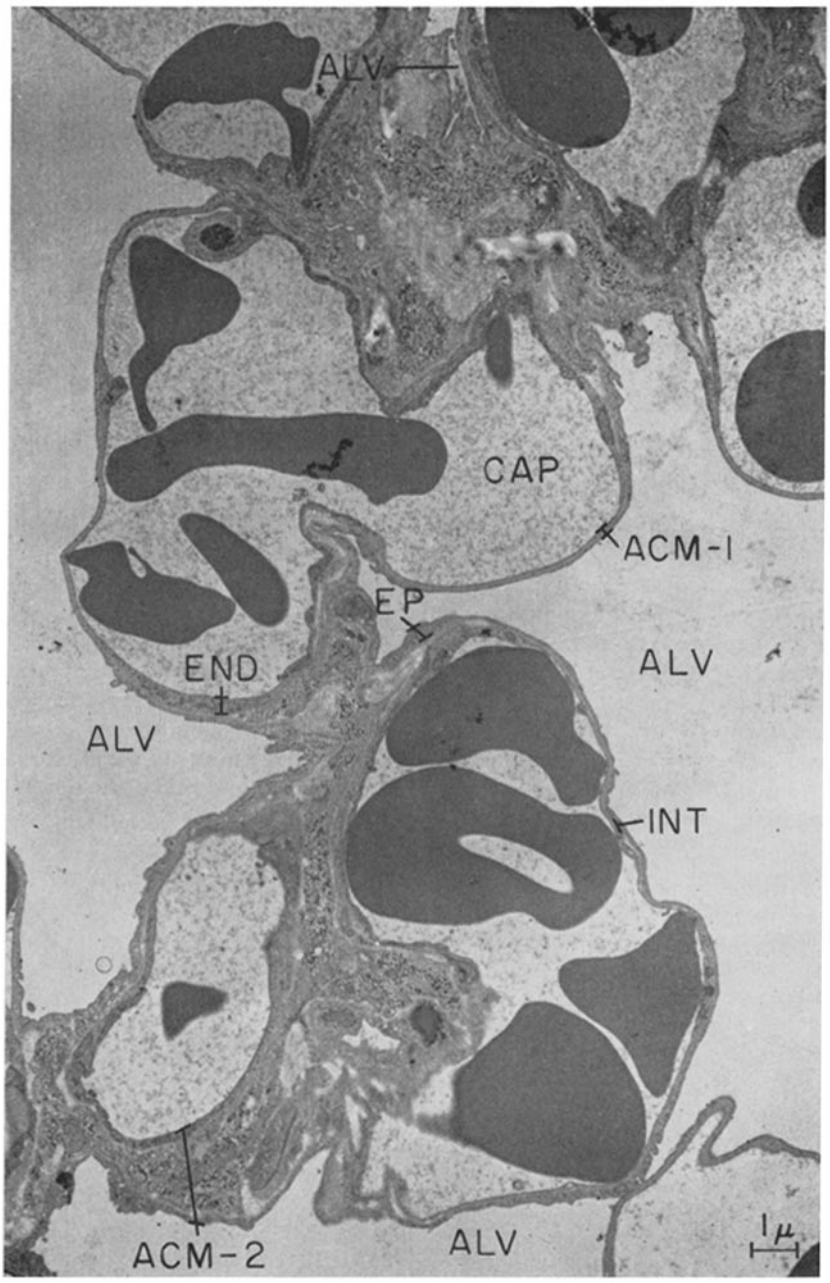

FIGURE 1 Section of septum between alveoli (*ALV*) containing a number of capillaries (*CAP*). Note the considerable variation in the thickness of the alveolo-capillary "membrane" (*ACM*) with alternating thin (*1*) and thicker (*2*) regions. The barrier is composed of an epithelial (*EP*), an endothelial (*END*), and an interstitial layer (*INT*). Rat lung. × 5,500.

estimated previously through measurements of the alveolar and capillary surface areas (8, 13, 14). Its composition has been studied elsewhere as well (8). In this paper, we wish to analyze its *thickness* inasmuch as this may contribute to a better understanding of the various functional events taking place in the periphery of the lung. As Figs. 1 and 2 show, the thickness of the alveolo-capillary mem-

brane varies considerably from place to place: thin and thick regions are found to alternate. The membrane thickness is never zero, nor is it infinite; it rather varies between some minimal and maximal thicknesses. It will first be shown that the mass of tissue building the barrier and determining oxygen consumption is reflected in the *arithmetic mean thickness* of the membrane, while the diffusion resistance is proportional to its *harmonic mean thickness*. The presentation of methods of measurement and of results obtained on rat lungs will be followed by a model analysis of the air-blood barrier, in which it will be shown that the diffusion resistance of the barrier appears to be minimized.

Definition of Characteristic Parameters

A. Thickness Determining Tissue Mass

It is evident that the mass of a sheet of tissue extending over an area S is proportional to the arithmetic mean thickness

$$\bar{\tau} = \int_a^b \tau \cdot F(\tau) \cdot d\tau \tag{1}$$

where a and b are the minimal and maximal thicknesses, respectively. $F(\tau)$ is the probability of measuring a thickness $a \leqq \tau \leqq b$.

B. Effective Thickness With Respect to Gas Diffusion

In order to derive the characteristic parameter for the effective thickness of a diffusion barrier, consider a prismatic piece of tissue of constant thickness τ and of cross-sectional area s (Fig. 4). It is in contact with air (A) on one side and with blood (B) on the opposite side. Assume a gas, say oxygen, to be present in both media with a constant partial pressure difference ΔP. Under equilibrium conditions, the flow of gas dQ across this slab of tissue in the unit time is, according to Fick's law,

$$dQ = D_M \cdot \Delta P \cdot \frac{s}{\tau} \tag{2}$$

where D_M is the diffusion coefficient of the tissue composing the barrier.

The thickness of the air-blood barrier of the lung (Fig. 5) is not constant but varies between a minimal thickness a and a maximal thickness b. Each thickness $a \leqq \tau \leqq b$ is present over an area $s(\tau)$ so that the sum of all $s(\tau)$ represents the total cross-sectional area S of the entire barrier. The over-all flow of the gas is then

$$Q = \int dQ = D_M \Delta P \int_a^b s(\tau) \cdot \frac{1}{\tau} \cdot d\tau \tag{3}$$

We assume here that the diffusion coefficient D_M and the pressure gradient ΔP vary independently of τ, which is true only in a limited sense, as discussed below. If we express

$$\frac{s(\tau)}{S} = F(\tau) \tag{4}$$

as the frequency or probability density of τ, then (3) becomes

$$Q = D_M \cdot \Delta P \cdot S \cdot \int_a^b d\tau \cdot \frac{1}{\tau} \cdot F(\tau) = \frac{D_M \cdot \Delta P \cdot S}{\tau_h} \tag{5}$$

From this we observe that the effective thickness of the barrier is its *harmonic mean thickness* τ_h, since

$$\frac{1}{\tau_h} = \int_a^b d\tau \cdot \frac{1}{\tau} \cdot F(\tau) \tag{6}$$

It should be noted that the harmonic mean thickness is weighted in favor of thin areas, while the arithmetic mean thickness is weighted in favor of thick areas; we therefore find that

$$\bar{\tau} > \tau_h \tag{7}$$

In the following account we will present special methods by which $\bar{\tau}$ and τ_h can be measured in the electron microscope.

Methods of Measurements

1. Principle for measuring the arithmetic mean thickness: The average half-thickness $\bar{\tau}_{1/2}$ of a double-faced tissue sheet such as the alveolo-capillary air-blood barrier can be defined as the average volume of tissue falling on the unit area of its surface (Fig. 6). For the purpose of analysis, suppose the tissue sheet to be contained in a cube of volume V; it has a volume $v = \eta \cdot V$ and a total surface area S, so that

$$\bar{\tau}_{1/2} = \frac{v}{S} = \frac{\eta \cdot V}{S} \tag{8}$$

This quantity can be conveniently measured by application of a principle proposed by Chalkley, Cornfield, and Park in 1949 (15). Its derivation has been presented in detail elsewhere (8, 16), so that we restrict ourselves to an outline of the essential points.

If a set of lines which have a combined length L is randomly placed through the cube, the surface of the tissue sheet will be cut by these lines n times, where

$$n = \frac{L \cdot S}{2V} \tag{9}$$

If this set is composed of Q short lines of equal length z, whereby $z << V^{1/3}$, then

$$n = \frac{Q \cdot z \cdot S}{2V} \tag{10}$$

With random distribution and orientation of these lines a number p of its $2Q$ end-points will lie within the tissue sheet. As was shown elsewhere (8, 16, 17)

$$p = \eta \cdot 2Q \tag{11}$$

By solving (10) for S and (11) for η and by substitution into (8), we find the double of the average half-thickness of the tissue sheet to be

$$\bar{\tau} = \frac{z \cdot p}{2n} \tag{13}$$

The air-blood barrier can be assumed to be randomly oriented within a cube of lung tissue as it is used for histological preparation (8, 16). It is cut at random by histological sections. Randomly projecting a suitable set of lines of length z on such a section thus amounts to randomly suspending them in the cube. By counting the number n of intersections with the internal and external barrier surfaces and the number p of end-points lying within the barrier, we can estimate its arithmetic mean thickness $\bar{\tau}$ from equation 13. Further practical details will be discussed below.

2. PRINCIPLE FOR ESTIMATING THE HARMONIC MEAN THICKNESS OF THE BARRIER FROM THE DISTRIBUTION OF INTERCEPT-LENGTHS: Consider the air-blood barrier to be broken up into N small flat plates of (circular) area a, and assume first a constant thickness τ. These plates can be oriented in any direction in space. Now let a set of long probing lines of length L, which are regularly spaced over a cross-section F, penetrate the system. These probes hit and cross the plates at an angle ϑ to their normals (Fig. 7). The probability that a given plate is hit by a probe is proportional to the projection area of the plate on F which is

$$f = a \cdot \cos \vartheta \tag{14}$$

(We consider only probes entering the "front face" of the plates.) On the other hand, the probability that the plates are inclined to the probes at an angle lying between ϑ and $\vartheta + d\vartheta$ is easily shown to be

$$R(\vartheta)d\vartheta = \sin \vartheta d\vartheta \tag{15}$$

The total number of penetrations of the probes at an angle lying between ϑ and $\vartheta + d\vartheta$ is, therefore,

$$Z(\vartheta)d\vartheta = \frac{a \cdot \cos \vartheta}{F} \cdot N \cdot L \cdot \sin \vartheta d\vartheta \tag{16}$$

If the plate thickness is τ the length of penetration of the probe, the intercept length, is

FIGURE 2 Electron micrograph of part of a capillary (*CAP*) containing an erythrocyte (*Ec*). It is separated from two alveoli (*ALV*) by an air-blood barrier (*ACM*) of varying thickness. The thick portion is here mainly occupied by the body of an endothelial cell (*END*) containing the nucleus (*N*), mitochondria (*M*), and other organelles. At the periphery (arrows) the cytoplasm becomes attenuated and can extend over large areas of the capillary wall. Only attenuated portions of epithelial cells (*EP*) are visible in this section. The interstitium (*INT*) contains the basement membranes (*BM*) of the epithelium and endothelium which appear fused in the thin portions of the barrier. Rat lung. × 22,000.

FIGURE 3 Detail of alveolo-capillary membrane in thin portion, showing the four plasma membranes of epithelial (*EP*) and endothelial (*END*) cells with the intercalated narrow interstitial space (*INT*) with fused basement membranes. Rat lung. × 140,000.

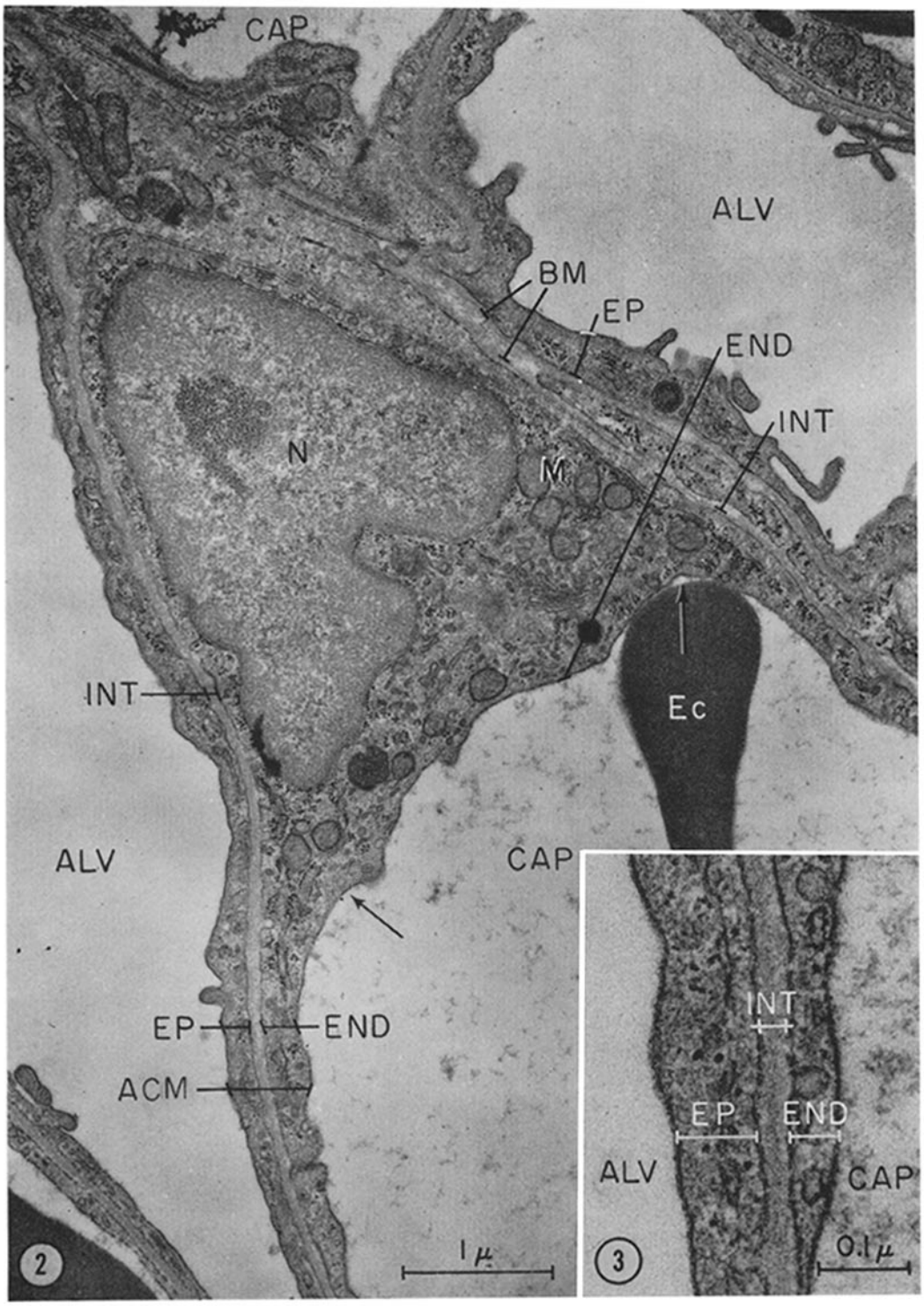
CAP
ALV
BM
EP
END
INT
N
M
Ec
INT
ALV
CAP
EP
END
ACM
1 μ
2
INT
EP
END
ALV
CAP
0.1 μ
3

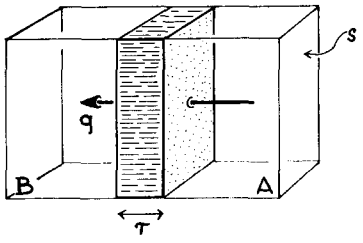

FIGURE 4

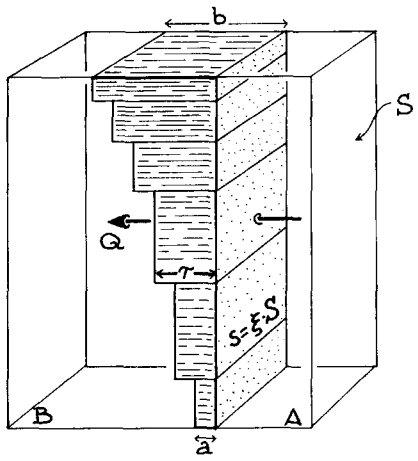

FIGURE 5

FIGURE 4 Model for deriving gas conductance through barrier of even thickness.
FIGURE 5 Model for deriving gas conductance through barrier of varying thickness. Compare text.

$$l = \frac{\tau}{\cos \vartheta} \tag{17}$$

The inverse of the harmonic mean l_h of these intercept lengths is, therefore,

$$\frac{1}{l_h} = \frac{\frac{N \cdot a \cdot L}{F} \cdot \int \frac{\cos \vartheta}{\tau} \cdot \cos \vartheta \sin \vartheta \, d\vartheta}{\frac{N \cdot a \cdot L}{F} \int \cos \vartheta \sin \vartheta \, d\vartheta} \tag{18}$$

$$= \frac{1}{\tau} \cdot \frac{\int \cos^2 \vartheta \cdot d(\cos \vartheta)}{\int \cos \vartheta \, d(\cos \vartheta)} \tag{19}$$

which gives

$$\frac{1}{l_h} = \frac{1}{\tau} \cdot \frac{2}{3} \tag{20}$$

If we allow the plate thickness to vary, we have Q sets of plates of thickness τ_i in the system, each one satisfying the above relations, and each one having a numerical weight w_i. For each set the harmonic mean l_{hi} of the intercept lengths is related to τ_i through equation (20). Therefore, the harmonic mean thickness of all plates in the system τ_h follows from

$$\frac{1}{\tau_h} = \sum_{i=1}^{Q} w_i \cdot \frac{1}{\tau_i} \tag{21}$$

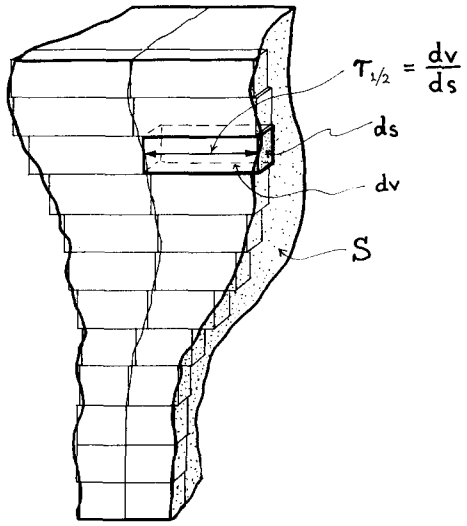

FIGURE 6 Definition of half-thickness of barrier.

$$= \sum_{i=1}^{Q} w_i \cdot \frac{3}{2l_{hi}} \tag{22}$$

and thus we find that

$$\tau_h = \tfrac{2}{3} \cdot l_h \tag{23}$$

where l_h is the harmonic mean of all intercept lengths of the probes, which may be calculated from measurements of l obtained directly in the electron microscope by the method outlined below.

In breaking up the air-blood barrier into small

flat plates for this derivation we may have introduced a certain error, since the natural barrier is continuously curved. In order to check on this we have conducted some model experiments with hollow foam-plastic cylinders of irregular wall thickness and a relative curvature which greatly exceeded that observed in the lung. By means of 550 equidistant measurements the harmonic mean thickness τ_h of the cylinder wall was found to be 9.39 mm. The cylinders were randomly embedded in plastic foam, and the resulting blocks were sliced with a band saw. A set of parallel lines was placed on all cut-surfaces and their intercept-lengths l across the cylinder walls were recorded. From 810 such measurements the harmonic mean

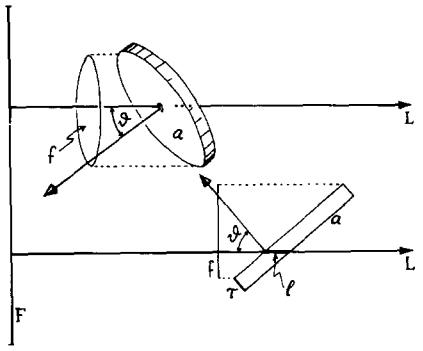

FIGURE 7 Model for deriving measuring principle for harmonic mean thickness. Compare text.

intercept-length l_h was found to be 13.82 mm. By applying equation (23), τ_h was thus estimated at 9.21 mm. The difference of 2 per cent between the measured and the estimated values of τ_h is inappreciable. This principle can thus be applied with confidence to the air-blood barrier in the lung.

This principle applies strictly only to infinitely thin sections of the barrier. The use of sections of finite thickness of some 0.06 μ may result in a slight overestimation of l in the thinnest regions of the barrier (where $\tau = 0.1$ μ) due to Holmes effect (16). In thicker parts of the barrier this effect from section thickness is negligible. On the other hand, the fact that l is measured in terms of units of length d by means of equidistantly spaced dots (see below) may introduce errors in both directions, since d is of the same order of magnitude as the minimal barrier thickness. These errors arise because small numbers of "hits" of the barrier by the dots (short values of l) are more affected by simple measuring errors than large numbers. However, these errors should not be very large and they may, in part, cancel each other. We have, therefore, abstained from correcting our results for possible systematic errors inherent in the method.

3. PRACTICAL APPLICATION OF THE MEASURING PRINCIPLES: Because of the small dimensions (0.1 to 5 μ in thickness) of the pulmonary air-blood barrier, its study requires the level of magnification and resolution provided by the electron microscope. Non-oriented ultrathin sections ($\sim$600 A) of lung tissue can be considered to provide two-dimensional random samples of the barrier (8, 13). The application of the measuring principles described above to a study in the electron microscope is, therefore, possible: in principle, random ultrathin sections of lung tissue are projected and observed on the fluorescent screen. The latter is provided with a lattice of lines (Fig. 8), by means of which the necessary measurements can be obtained.

This lattice incorporates a system of 15 lines of equal length $z = 1.2$ cm; their end-points form a regular hexagonal point network. This ensures that the end-points are evenly distributed over the entire field and avoids any bias that might be introduced by the presence of lines connecting some of the points. Such a hexagonal network is ideally suited for point-counting volumetry (17, 16) which is involved in the determination of $\bar{\tau}$. The lines are oriented in three directions; this is desirable because neither section nor screen can be rotated. The measurements necessary for determining the arithmetic mean barrier thickness $\bar{\tau}$ are simple counts of the number n of intersections of the lines with the external and internal surfaces of the barrier, and the number p of end-points lying on the tissue. They are easily recorded on a differential counting device as used, for example, in hematology.

The determination of the harmonic mean barrier thickness necessitates the measurements of the intercept length l of a random probing line crossing the barrier. To facilitate this measurement, eight parallel rows[1] of equidistant dots have

[1] The use of eight parallel probes (rows of dots) in one setting is a matter of convenience. It should be noted that the probes are widely spaced. By virtue of the curvature of the barrier, each probe intercepts the barrier at a different angle ϑ (Fig. 8), so that we are, in effect, using eight independent probes.

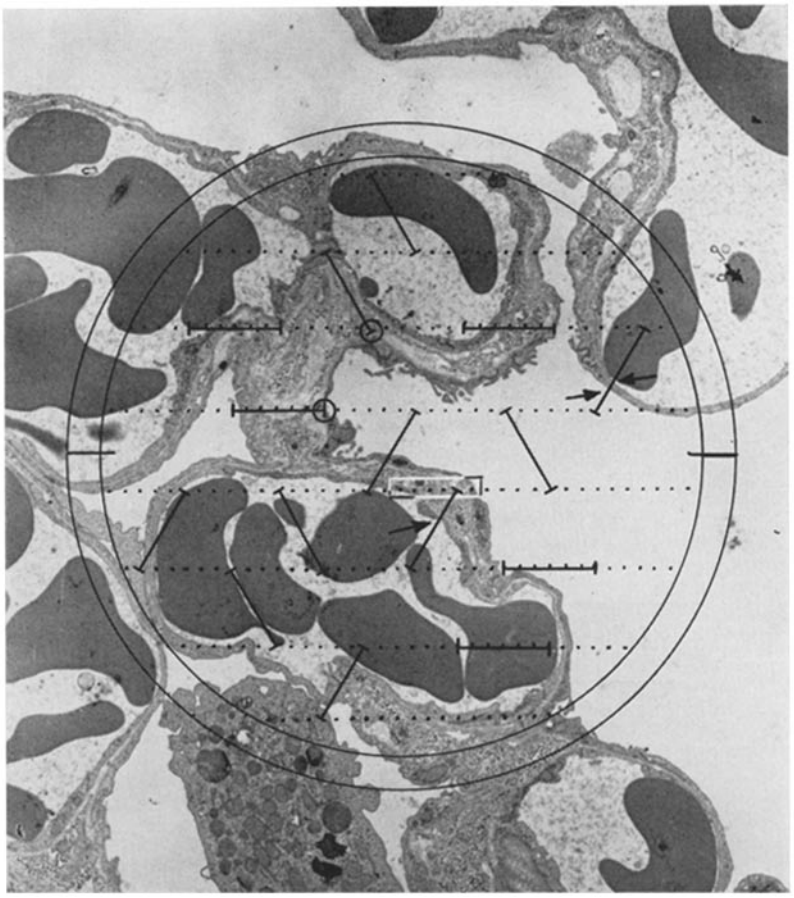

FIGURE 8 Electron micrograph of random sample section of rat lung showing position of lattice of measuring lines described in text. Rectangle marks a row of dots used in measuring intercept length l. Arrows point at intercept of short measuring line with barrier surface. Circle indicates end-point lying on tissue.

been marked on the screen (Fig. 8). It was found convenient to space the dots at a distance d = 0.2 cm. By counting the number m of dots which lie on a section of the barrier we find the intercept length $l = m \cdot d$. To avoid an overestimation of l by this procedure, dots which touch the left surface of the barrier are disregarded, while those touching the right surface are counted. In Fig. 8, a typical field of a random section of the rat lung has been superimposed with the lattice as it was engraved into the phosphor of the fluorescent screen of a Siemens Elmiskop I. Examples of endpoints of the short sampling lines lying within the barrier have been marked by a circle, examples of intersections with the surface by an arrow. A row of dots illustrating the measurement of l is surrounded by a rectangle.

MATERIAL AND METHODS OF PREPARATION

The above morphometric principles were applied to the measurement of the thickness of the air-blood barrier in three rat lungs, which were fixed by two different procedures under deep Nembutal anesthesia: The first specimen (R8) was fixed *in situ* by intratracheal instillation of 1.5 ml of 1 per cent OsO_4 buffered at pH 7.4 in 0.1 M potassium phosphate buffer. Ten minutes after instillation, the fixed parts of the lung were cut into 100 to 200 small blocks of 2 to 3 mm^3 which were left in the fixative for 2 hours under vacuum and in ice. The two other specimens were fixed by instillation of 6 per cent glutaraldehyde in 0.1 M potassium phosphate buffer (pH 7.4) according to the method of Sabatini *et al.* (18). This method led to a rapid stiffening of the delicate lung tissue so that blocks could be cut without appreciable

distortion. After 2 hours' fixation in the cold and under vacuum, the blocks were washed for 2 hours in cold buffered sucrose and refixed for 2 hours in 1 per cent OsO_4 in the same buffer. Subsequently, the blocks were dehydrated in alcohol and infiltrated with Epon 812 (19). After primary sampling (see below), the selected blocks were sectioned on an LKB Ultrotome using a Dupont diamond knife. The sections were about 1 to 1.5 mm wide and 2 to 2.5 mm long, and were cut about 600 to 800 A thick (silver-gold). They were mounted on 400-mesh copper grids on a thin carbon-coated Formvar film and contrasted with lead by the method B of Karnovsky (20).

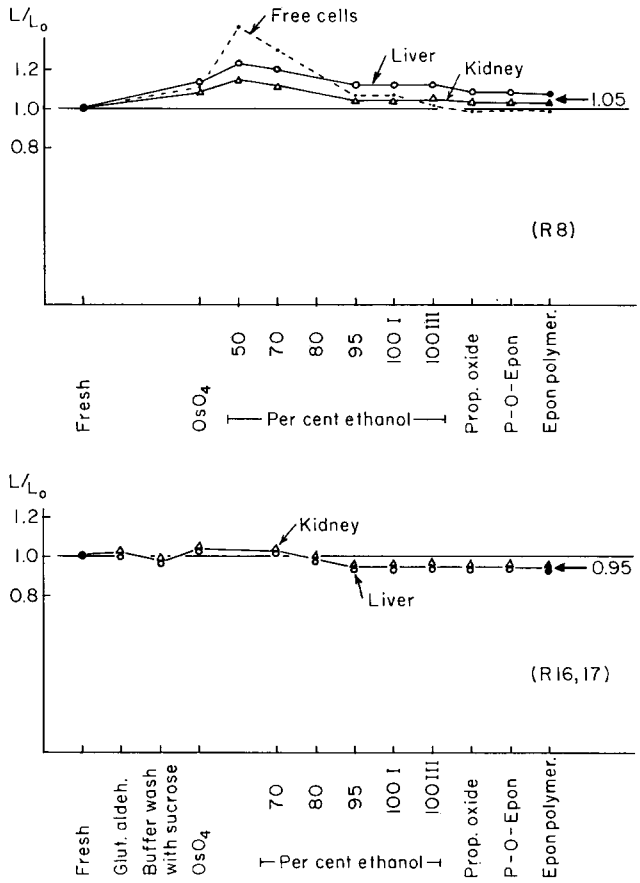

FIGURE 9 Relative dimensions (L/L_o) of tissue blocks and free culture cells during fixation, dehydration, and embedding, according to two different techniques. Compare text.

ARTIFICIAL CHANGES IN TISSUE DIMENSIONS OCCURRING WITH PREPARATION

The influence of the fixing, dehydrating, and embedding agents may introduce some changes in dimensions of tissue structures from the fresh to the processed specimen. This must be considered in interpreting, with respect to the fresh (living) lung, dimensions measured on histologic sections. The degree of dimensional change caused by our technique was, therefore, investigated in a series of test experiments. Since the flaccidity of lung tissue did not allow reliable direct measurements on the blocks during processing, these studies were carried out on blocks of liver, kidney, and sclera, and, in part, on free cells cultured in suspension.

A. *OsO_4 Fixation (Case R8)*

As reported earlier in detail (8), it was found that fixation with "isotonic" phosphate-buffered OsO_4 induced a slight swelling of cells and tissues (Fig. 9). An appreciable increase in the average linear dimensions of cells and tissues occurred at the beginning of dehydration in 50 per cent ethanol. The average volume of free cells increased by a factor of 2.8, that of liver blocks and kidney

by 1.9 and 1.5, respectively. The dimensions of sclera blocks remained unchanged. It is thus probable that this swelling was due to an osmotic effect. After dehydration, infiltration, and embedding, the dimensions of the free cells were about equal to those measured in the fresh state, but the final dimensions of embedded liver and kidney blocks were still about 5 per cent larger than those measured in the fresh state.

B. *Glutaraldehyde Fixation (Cases R16 and R17)*

Because of these observed drastic dimensional changes, a different method was adopted in the preparation of the subsequent lungs. The lungs of the anesthetized animals were fixed *in situ* by instillation of phosphate-buffered glutaraldehyde (18) into the airways. The dimensions of liver and kidney blocks fixed in this solution did not change significantly (Fig. 9). After washing in a buffered sucrose solution the blocks were refixed in buffered OsO_4 which again induced a slight swelling by some 6 per cent linearly. By initiating dehydration in 70 per cent alcohol, no further swelling of the tissues occurred. Subsequent dehydration and infiltration reduced the block dimensions by some 8 per cent, so that the final dimensions were about 5 per cent smaller than those measured in the fresh state.

TABLE I

Artificial Changes in Tissue Dimensions Due to Processing

Data of liver and kidney pooled

Final relative dimensions:		
OsO_4 fixation	o	= 1.056
Glutaraldehyde fixation	g	= 0.953
$d = o - g$		= 0.103
Statistical tests:		
Degrees of freedom	ν	= 28
$t = d/s_{\nu d}$		= 5.28
Significance of d:	P	< 0.0005
Conversion coefficients to fresh dimensions:		
OsO_4 fixation	$1/o$	= 0.96
Glutaraldehyde fixation	$1/g$	= 1.05

C. *Difference between the Two Procedures*

Assuming that the effect of these preparative procedures on the tissue of the pulmonary air-blood barrier lies between those observed for the kidney and the liver, we can expect on the basis of these experiments that the dimensions measured in the lung R8 should be about 10 per cent larger than those determined in the lungs R16 and R17. Table I compares the two final relative dimensions for the pooled data on liver and kidney. The difference $d = 0.103$ was found to be statistically highly significant (Table I). We have, therefore, derived a pair of coefficients which allow conversion of the linear dimensions measured on sectioned tissue of both groups to those pertaining to the fresh tissue. For osmium tetroxide-fixed material, with 50 per cent ethanol used as the initial dehydrating agent, this coefficient is 0.96; for the glutaraldehyde-fixed tissue, dehydrated initially in 70 per cent ethanol, it is 1.05.

METHOD OF RANDOM SAMPLING

Particular care was taken to draw an unbiased random sample by a two-stage random sampling procedure. The 100 to 200 tissue blocks obtained from chopping the part of the lung fixed by instillation of the fixative were arrayed in a flat dish over a piece of square paper whose squares had been numbered consecutively. By means of a table of random numbers, four times five blocks were chosen for embedding. The first group of five represented the primary sample which was sectioned and subjected to our analysis; the other blocks were kept as reserves.

In the second sampling stage a random sample of five fields was selected on each section, again by means of random number tables. For this purpose the squares of the 400-mesh grids accessible for investigation were drawn out on a master sheet and numbered consecutively (8). The studies being executed in a Siemens Elmiskop I, the grids were sampled on the intermediate screen. Upon slight defocusing of the second condenser lens a typical (marginal) square was easily located. By enumeration of squares the grid was scanned and the position of the section—visualized by a darkfield effect around the small objective aperture—was marked on the master sheet. Five numbers, read off a random number table, located the squares to be investigated. If these squares did not contain sections of the barrier they were discarded, and new squares were selected.

After location of each sample square, the condenser was focused and the measurements were obtained on the main screen at a magnification of × 3,900. On each square the line system of Fig. 8 could be placed four times. To avoid bias in positioning the lattice, its inner circle was made to be tangent to two sides of each corner of the square.

RESULTS

1. *Arithmetic Mean Thickness* $\bar{\tau}$

By the above-stated procedure a total of 1500 lines of length $z = 3.2\ \mu$ with 3000 end-points was randomly suspended in the lung tissue. According to equation 13, the mean thickness $\bar{\tau}$ followed from the number n of intersections of these lines with the alveolar and capillary surfaces of the barrier and from the number p of end-points lying within the tissue space. Table II presents the findings on the three investigated rat lungs. The average of the ratio p/n was found to be 0.93 in R8, and 0.75 in the lungs R16 and R17. Fig. 10 shows the plots of the cumulative average of p/n for the successive samples. In the second half of the curve, strong deviations in the individual values of p/n do not cause significant changes in the average value. The relative standard error of the mean was found to be of the order of 8 to 10 per cent, which is considered satisfactory for the present purpose. The arithmetic mean thickness of the fixed and processed barrier was about 1.2 μ for cases R16 and R17 which were fixed with glutaraldehyde, and 1.3 μ for case R8 which had been fixed with OsO_4. After conversion of these dimensions to the fresh state by means of the respective correction factors (*cf.* above), the final values of $\bar{\tau}$ of all three cases compared well with each other. Their average value was 1.25 μ.

TABLE II

Mean Dimensions of Barrier

Rat	p	n	$\langle p/n \rangle$	SE	$\bar{\tau}\,\mu$	$l_h\,\mu$	$\tau_h\,\mu$	linear corr. to fresh	$\bar{\tau}'\,\mu$	$\tau_h'\,\mu$	$\bar{\tau}/\tau_h$
R8	538	619	0.93	±0.09	1.30	0.92	0.61	0.96	1.25	0.58	2.2
R16	535	715	0.75	±0.06	1.16	0.82	0.55	1.05	1.22	0.58	2.1
R17	495	622	0.74	±0.07	1.23* (1.15)‡	0.78	0.52	1.05	1.29* (1.21)‡	0.55	2.3* (2.1)‡
						Group average:			1.25	0.57	2.2

* Computed from pooled data p and n.
‡ Computed from average ratio p/n.

2. *Harmonic Mean Thickness* τ_h

The harmonic mean thickness τ_h was calculated from the harmonic mean intercept-length l_h of random probing lines traversing the barrier according to equation (23). The histograms of Fig. 11 present the distribution of the intercept length l measured on some 700 random probing lines in the specimens R16 and R17. The values of l_h were about 0.8 μ, and τ_h was, therefore, found to be 0.55 μ (Table II). In case R8, l_h and τ_h were somewhat larger. After conversion of these dimensions to those pertaining to the fresh state (*cf.* above), the values of τ_h found in the three cases compared well with each other and had a group average of 0.57 μ.

3. *Minimal and Maximal Barrier Thicknesses*

In the subsequent analysis, it will be necessary to have an estimate of the minimal barrier thickness a, or more precisely of some "average minimal thickness." This could obviously not be accurately determined, since it is not the same in all "thinnest regions." From direct measurements on electron micrographs it could, however, be derived that the most frequently occurring minimal thickness lies between 0.1 and 0.25 μ, the average being about 0.15 μ. This estimate is sufficient for our present purpose.

The maximal thickness of the barrier b is more difficult to define and to assess. It might most frequently correspond to the thickest portions of alveolar epithelial cells, which are of the order of 4 to 8 μ. However, in the further analysis no reliable estimate of b will be necessary.

4. *Volumetric Composition of Barrier*

As an additional result of this study, the relative volumes of the major components of the barrier,

i.e. alveolar epithelium, interstitium, and capillary endothelium, could be determined by differential point counting (8, 16, 17). The end-points of the short sampling lines lying on these structures were recorded separately; the relative numbers of points thus obtained correspond to the relative volumes. Table III shows that the distribution of these components was found to be very consistent in all three cases. The interstitium occupied about 40 per cent, and each cellular layer some 30 per cent of the barrier space.

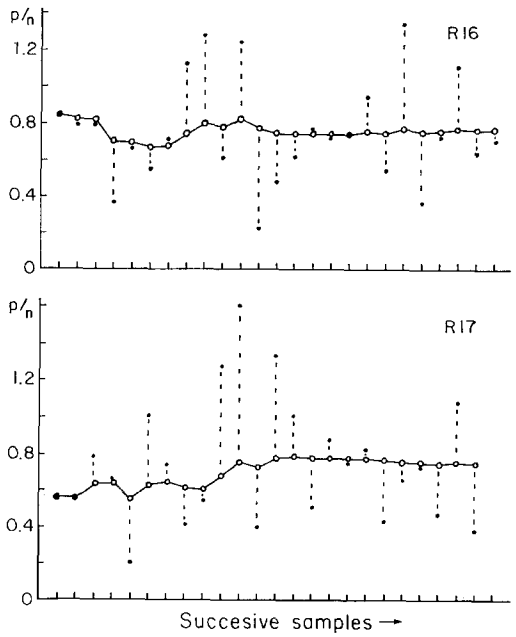

FIGURE 10 Cumulative averages (open circles) of ratio p/n used in estimating $\bar{\tau}$. Dots mark values measured on individual samples.

As an indirect check on the quality of the samples investigated, we have also determined, by the same procedure, the relative volumes of barrier tissue and capillary blood, *i.e.* the fractions they occupy in the space of the interalveolar septa. It was consistently found that the tissue amounted to some 36 per cent, the blood occupying 64 per cent. These figures are affected by a relative probable error of 1.3 per cent in all three cases, the absolute probable error being about 0.5 per cent. This good result gives us further confidence in the barrier dimensions obtained on these samples.

A MODEL FOR THE ALVEOLO-CAPILLARY BARRIER

In order to discuss the functional implications of the measurements presented above, a model for the air-blood barrier will now be constructed. It is a model in the sense that it is *not* intended to display *all* features of the barrier quantitatively, but rather furnish further insight into a few of its important properties. The model membrane chosen is a structure of periodic ripples shown in Fig. 15. This structure has a mean thickness $\bar{\tau}$, a harmonic mean thickness τ_h, closely related to its gas impedance, a minimum thickness a, all directly obtainable by electron microscopy and the methods discussed above. A mathematical form may be chosen for the configuration of the ripple:

$$Z(\tau) = \frac{\lambda}{2\pi}\left\{\arcsin\frac{(\tau - a) - (b - \tau)}{b - a} - \beta\sqrt{(\tau - a)(b - \tau)} + \tfrac{1}{2}\right\} \tag{24}$$

This is shown in Fig. 12 for several values of β. In the expression above, λ is the wavelength of the ripples, and b is their maximum height. This mathematical form has been chosen for two reasons: (1) It yields a family of configurations, one of which should fairly closely resemble the figure of the natural air-blood barrier, and (2) It permits direct evaluation of $\bar{\tau}$ and τ_h.

The probability density for thicknesses τ in such a model is easily seen to be

$$P(\tau) = \frac{1}{Z(b) - Z(a)} \cdot \frac{d}{d\tau} Z(\tau) \tag{25}$$

from which the arithmetic and harmonic mean thicknesses may be evaluated straightforwardly as

$$\bar{\tau} = \frac{a + b}{2} + \beta\frac{\pi}{2}\left\{\left(\frac{a + b}{2}\right)^2 - ab\right\} \tag{26}$$

and

$$\frac{1}{\tau_h} = \frac{1}{\sqrt{ab}} - \beta\pi\left\{\frac{a + b}{2\sqrt{ab}} - 1\right\} \tag{27}$$

These results give a ratio of means

$$\frac{\bar{\tau}}{\tau_h} = \frac{u}{g} + \beta\pi\left(u - \frac{u^2}{2g} - \frac{g}{2}\right) - \tfrac{1}{2}\beta^2\pi^2\left\{(u^2 - g^2)\left(\frac{u}{g} - 1\right)\right\} \tag{28}$$

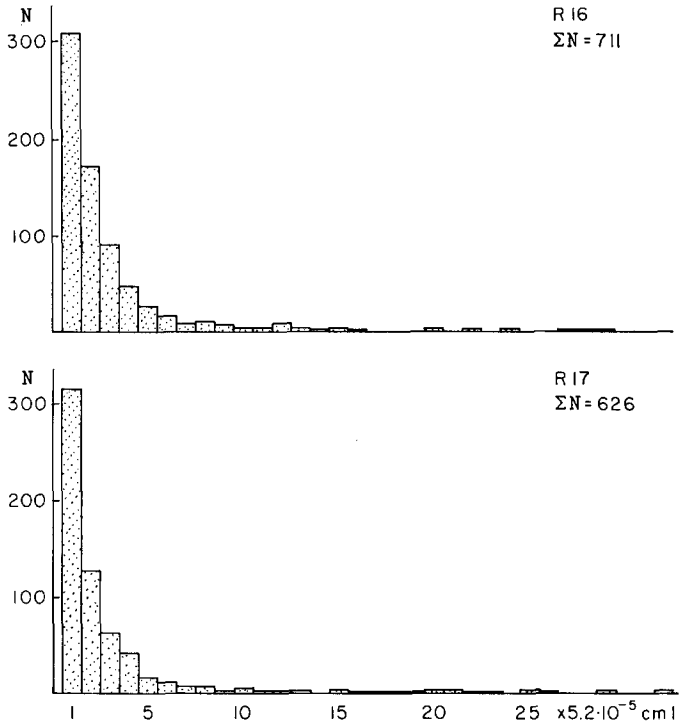

FIGURE 11 Histograms of length l of random probing line.

TABLE III

Volumetric Composition of Barrier and Interalveolar Septum

Rat	Epithelium	Interstitium	Endothelium	Blood	Tissue	P.E. (relative with respect to tissue)
R8	0.32	0.41	0.27	0.63	0.37	0.014
R16	0.31	0.40	0.29	0.64	0.36	0.013
R17	0.28	0.42	0.30	0.64	0.36	0.013

where

$$u = \frac{a+b}{2} \quad \text{and} \quad g = \sqrt{ab} \tag{29}$$

In principle, if both the minimum thickness a and the maximum thickness b were known, as well as the experimentally determined ratio $\bar{\tau}/\tau_h$, equation (28) could be solved as a quadratic for β, which would complete the determination of the membrane model. However, b is not readily accessible to experiment, as discussed above. Hence another approach was used to determine β.

The equations (26) to (28) may be expressed in terms of dimensionless variables, by means of measuring distances in units corresponding to the minimal thickness a. Thus, let the dimensionless variables be

$$b' = \frac{b}{a}, \quad \bar{\tau}' = \frac{\bar{\tau}}{a}, \quad \beta' = a\beta \tag{30}$$

whence

$$u' = \frac{1+b'}{2}, \quad g' = \sqrt{b'}. \tag{31}$$

The dimensionless mean thickness becomes

$$\bar{\tau}' = u' + \beta' \frac{\pi}{2} \{u'^2 - g'^2\} \tag{32}$$

and the quadratic for β'

$$\frac{\bar{\tau}}{\tau_h} = \frac{u'}{g'} + \beta'\pi \left\{ u' - \frac{u'^2}{2g'} - \frac{g'}{2} \right\} - \frac{1}{2}\beta'^2\pi^2 \left\{ (u'^2 - g'^2) \left(\frac{u'}{g'} - 1 \right) \right\} \tag{33}$$

In these equations, u' and g' are functions of the variable b' ($= b/a$) alone. The ratio $\bar{\tau}/\tau_h$ being known from our measurements, β' can now be found from solving the quadratic (33); it is a function of the only variable b'. Substitution into (32) yields $\bar{\tau}'$ which is again a sole function of b', and from it we find $a = \bar{\tau}/\bar{\tau}'$, the dimensional value of $\bar{\tau}$ being known from our measurements. It thus remains only to choose a value of b' so that the calculated value of a agrees with the observed minimal thickness, and the model has been completely defined, including the previously unknown maximal thickness $b = a \cdot b'$. Now this model system is subject to two important mathematical and physical constraints.

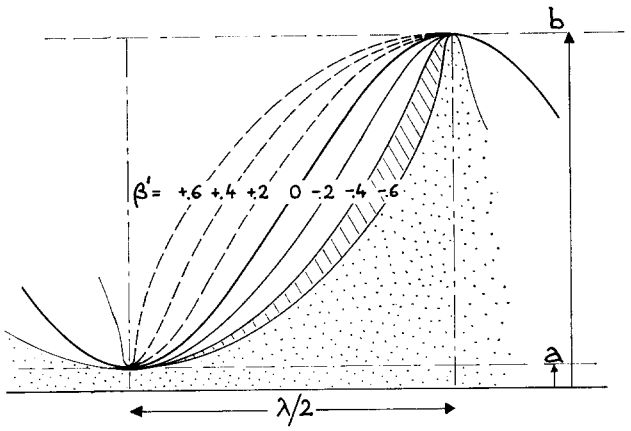

FIGURE 12 Effect of variation of coefficient β on configuration of dimensionless barrier model. Hatched area indicates possible range of configuration.

1) As β becomes more negative (with a and b fixed), the figure becomes one of wide valleys and slender peaks (Fig. 12) and the ratio $\bar{\tau}/\tau_h$ becomes *larger*. That is, the membrane gas conductance improves for a given expenditure of biological material measured by $\bar{\tau}$. However, if $-\beta$ exceeds $\frac{2}{\pi\,(b\,-\,a)}$ (the "sharp peak" value of β), then τ is no longer a single-valued function of Z, and the surface configuration becomes structurally absurd. Thus the lower limit of β is

$$\beta_{\min} = -\frac{2}{\pi(b' - 1)} \tag{34}$$

2) Evidently the harmonic mean thickness cannot be as small as the minimum thickness, nor the arithmetic mean thickness as large as the maximum thickness, whence

$$\frac{\bar{\tau}}{\tau_h} < b' \tag{35}$$

There is a largest accessible value of $\bar{\tau}/\tau_h$ for any fixed b'. Equivalently, if too small a value of b' is chosen in the quadratic for β, with $\bar{\tau}/\tau_h$ fixed, then no real solutions will exist: the solutions will be complex.

These two constraints reduce the possible choices of the remaining free variable b' (Table IV). For

TABLE IV

Parameters of Barrier Model in Possible Range with Measured Ratio $\bar{\tau}/\tau_h = 2.2$ and $\bar{\tau} = 1.25\ \mu$

$\beta'(b' - 1)$	$\bar{\tau}'$	$a = 1.25/\bar{\tau}'$	b'	b	β'
		μ		μ	
−0.35*	6.83	0.18	17	3.06	−0.022
−0.5	6.52	0.19	19	3.61	−0.028
−0.6‡	6.20	0.20	21	4.20	−0.031

* Limit by complex solutions.

‡ Limit by $\beta'_{\min}(b' - 1) = -\frac{2}{\pi}$.

the experimentally observed value of $\bar{\tau}/\tau_h = 2.2$ in the rat lung (Table II) the quadratic for β falls between these limiting criteria only in the range $21 \geqq b' \geqq 17$. To this corresponds a range of $6.2 \leqq \bar{\tau}' \leqq 6.83$ for the dimensionless arithmetic mean thickness of the barrier model, as derived by equation 32. And from the observed average thickness $\bar{\tau} = 1.25\ \mu$ (Table II), we derive the range of possible minimal thicknesses as $0.18\ \mu \leqq a \leqq 0.20\ \mu$, and for the maximal thickness $4.20\ \mu \geqq b \geqq 3.06\ \mu$. It can be observed that these model values of a and b agree very well with the minimal and maximal values observed in the rat lung by direct measurements on electron micrographs.

Since there is evidently no single minimal or maximal value in the natural barrier, it is not necessary to arrive at a choice of one specific pair of extreme dimensions for the model barrier. The ranges indicated above enclose a family of models, having identical tissue mass and gas conductance, which conform with the data obtained from measurements.

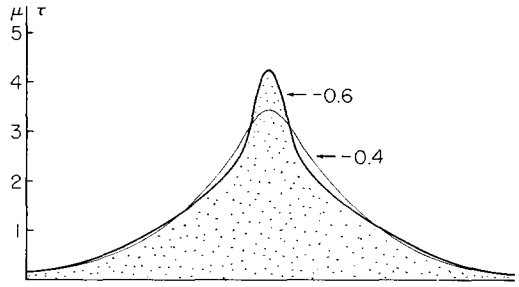

FIGURE 13 Configuration of cross-section of barrier models limiting the possible range. Note that modifications affect mainly the "hills."

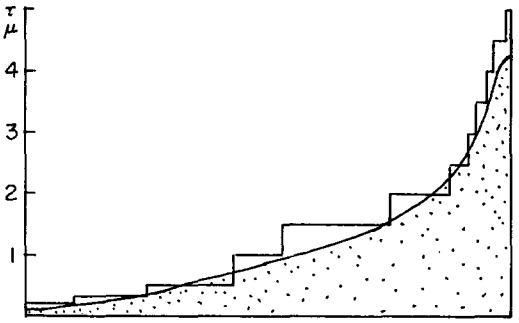

FIGURE 14 Half-period of model superimposed with histogram of distribution of barrier thickness secured from independent measurements (reference 8).

In Fig. 13, the cross-sections of one wave of each of the two limiting models are compared. It is easily seen that the configuration is not appreciably different in the two limiting examples. In Fig. 14, one half-wave of one of the models is shown plotted against the histogram of barrier thicknesses obtained by direct measurements on electron micrographs of a rat lung reported previously (8). It will be noted that the over-all agreement is excellent, so that this model can be regarded as a faithful representation of the natural air-blood barrier in the rat lung.

DISCUSSION

The dimensions of the alveolo-capillary membrane or air-blood barrier are of interest to physiologists in various respects: on the one hand, they will determine the degree of resistance which the barrier may offer to gases diffusing from air to blood, and on the other, they will be related to the amount of metabolic activity to be expected at this critical place (12). These dimensions can only be obtained in a reliable fashion by a morphometric study in the electron microscope. Earlier determinations of the barrier thickness (1–6) were based on single and selected measurements on electron micrographs and were usually restricted to an indication of some range of thickness in the "thin portions" of the barrier. A good set of measurements of this kind was given by Meessen (11) for various species. These studies, however, disregarded an important part of the barrier, its "thicker regions," and hence were of quite uncertain value.

In this paper, two methods have been presented by which the arithmetic and the harmonic mean thicknesses of the barrier could be measured directly on the screen of an electron microscope in a simple and efficient way. The measurements were obtained by random sampling procedures; hence no selection of measuring sites was necessary. The dimensions thus obtained qualified as true averages referring to the total barrier, and their statistical significance could be tested. The application of these methods to three normal rat lungs has also shown that the reproducibility of the results is very satisfactory.

By these methods, it was found that the arithmetic mean thickness of the air-blood barrier of rat lungs measures about 1.25 μ. This dimension is an estimate of the amount of tissue present on the square-centimeter of the barrier surface. It could be shown simultaneously that 30 per cent of this tissue consisted of alveolar epithelial cells and 30 per cent of capillary endothelial cells; 40 per cent belonged to the interstitium. These findings are of interest inasmuch as they can contribute to an assessment of the relative amount of oxygen consumed in the barrier tissue while this gas is diffusing from the alveolar air into the pulmonary capillary blood. Under normal circumstances, this quantity cannot yet be detected by physiological methods, while it can be measured in pathological cases with exaggerated tissue metabolism in the lung, as in pulmonary tubercu-

losis (12). However, before reliable calculations can be based on our findings, further knowledge on the quantitative relationship between metabolism and morphology of tissues is necessary.

The second method revealed that the harmonic mean barrier thickness of the rat lung measures about 0.57 μ. This dimension stands in direct relation to the diffusion resistance of the barrier. It is the characteristic over-all barrier thickness which has to be used in calculating theoretical values for the "membrane diffusing capacity" of the physiologists (9, 10, 21). No numerical calculations can be made at this time, since nothing is known as yet about the diffusion characteristics of the barrier tissues.

However, a structural feature of the pulmonary air-blood barrier which is functionally most interesting was revealed from these data when the form of the barrier was analyzed by means of a mathematical model. It was first observed that the natural barrier showed alternating thin and thick regions (Fig. 1). A mathematical model representing a rippled membrane was, therefore, chosen to represent it (Fig. 15); this model yielded a family of configurations, one of which should fairly well simulate the natural barrier, and it permitted a thorough mathematical analysis of its features. In this model, a coefficient β (*cf.* equation 24) determines the relative importance of hills and valleys (Fig. 12). In general, it was found that the more negative β became, the larger was the relative gas conductance of the barrier, measured by the ratio $\bar{\tau}/\tau_h$. We have defined two mathematical and physical constraints for this model, particularly a minimal value for β, its "sharp peak value."

Now there are some biological conditions which do not allow the barrier to reduce its thickness indefinitely. For one, the barrier has to secure a constant spatial relationship between air and blood; that is, it must have some minimal mechanical strength. This largely determines the minimal thickness a which was observed to be of the order of 0.1 to 0.2 μ in the rat lung, and to some extent the mass of tissue or the mean thickness $\bar{\tau}$. The maintenance of the integrity of the alveolo-capillary membrane, and some additional metabolic functions which this tissue may have, call for a minimum amount of cellular material to be present on the square centimeter of the membrane surface, and this determines largely the value of the mean thickness $\bar{\tau}$.

Hence, given a "membrane" of irreducible minimal thickness a and with an irreducible minimal amount of tissue per unit area measured by $\bar{\tau}$, it may be easily seen that the gas conductance of this system, estimated by $1/\tau_h$, is maximal when β has assumed its minimal value. In Fig. 16, the rippled membrane model with $\beta_{\min}$ is compared with a membrane of homogeneous thickness. The

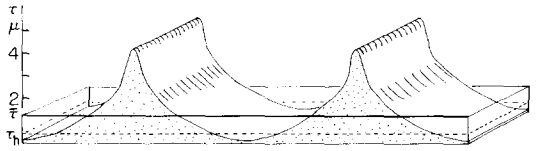

FIGURE 15 Three-dimensional representation of two periods of the barrier model. Volume of tissue ($\bar{\tau}$) and diffusion effective thickness (τ_h) are indicated.

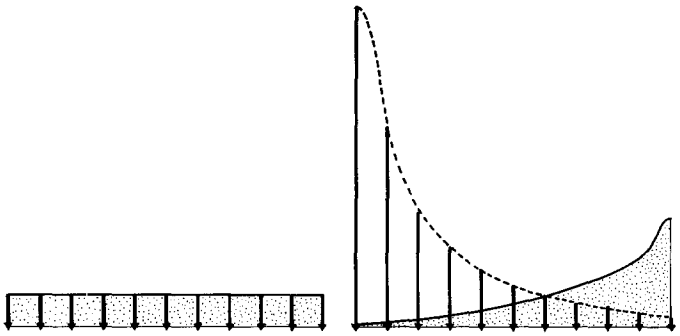

FIGURE 16 Effect of configuration of barriers of equal mass on gas conductance. Compare text.

gas conductance at every point is proportional to the arrow length. It can be seen that the over-all gas conductance of the rippled model is 2.2 times larger than that of the smooth membrane.

It was shown above that with a measured ratio $\bar{\tau}/\tau_h = 2.2$, only a small range of the model family was physically possible (Figs. 12 and 13), and that this corresponded to the range close to $\beta_{\min}$. Moreover, the minimal and maximal thicknesses as well as the general configuration of these models agreed well with observations made directly on the natural barrier (Fig. 14). This suggests that the gas conductance of the pulmonary air-blood barrier of the rat lung is nearly optimal, if we consider its minimal thickness and the mass of tissue to be given features which cannot be further reduced because of other biological conditions.

This optimization is achieved by concentrating the bulk of tissue in the thicker regions. The exact configuration of these parts of the barrier does not appear to be important; Fig. 13 shows that the possible configurations of the model having identical physical characteristics differ only in the configuration and height of the "hills," while the thin part is essentially identical in all examples. But Fig. 16 shows that the thicker half of the barrier accounts for only 15 per cent of the over-all gas conductance.

These studies have been done on rat lungs, and the figures refer to this species only. The air-blood barrier of man, in particular, will differ from that of the rat in various respects: the minimal thickness is larger, and it appears that the over-all thickness may also assume higher values. But before the human barrier can be quantitatively defined in a reliable fashion further studies are needed.

In addition, it will be necessary to determine the fractional composition of the barrier along the diffusion path. This will help to better understand diffusion characteristics of the barrier tissue. Here it should be pointed out that the diffusion coefficient D_M will most probably not be the same in all regions of the barrier. As was previously shown (8), so called discontinous components of the tissue are vastly concentrated in the thick regions (*cf.* Fig. 2). Special attention has also to be given to the dimension of a fluid film which is postulated to coat the surface of the alveolar epithelial cells, but so far, this film could not be demonstrated morphologically. When all of this is done, the data obtained through the methods proposed here can be used to calculate theoretical values for the "diffusing capacity" of the pulmonary air-blood barrier, and these can then be correlated with data ascertained by physiological methods on the living subject.

The authors wish to thank Dr. George E. Palade for generous support of this work and for many contributions to its successful pursuit, and to Dr. Domingo M. Gomez, Dr. August Hennig, and Professor B. L. van der Waerden for numerous valuable discussions.

This work was supported by an Investigatorship Grant (I-188) from the Health Research Council of the City of New York to Dr. Weibel.

Received for publication, July 23, 1963.

BIBLIOGRAPHY

1. Low, F. N., The pulmonary alveolar epithelium of laboratory mammals and man, *Anat. Rec.*, 1953, **117**, 241.
2. Karrer, H. E., Ultrastructure of mouse lung; general architecture of capillary and alveolar walls, *J. Biophysic. and Biochem. Cytol.*, 1956, **2**, 241.
3. Bargmann, W., and Knoop, A., Vergleichende elektronenmikroskopische Untersuchungen der Lungenkapillaren, *Z. Zellforsch.*, 1956, **44**, 263.
4. Policard, A., Collet, A., and Pregermain, S., Apports de la microscopie électronique à la connaissance histophysiologique de la paroi alvéolaire, *J. Physiol.* Paris, 1956, **48**, 687.
5. Policard, A., Collet, A., and Pregermain, S., Recherches au microscope électronique sur les cellules pariétales alvéolaires du poumon des mammifères, *Z. Zellforsch.*, 1959, **50**, 561.
6. Schulz, H., The submicroscopic anatomy and pathology of the lung, Berlin-Göttingen-Heidelberg, Springer, 1959.
7. Low, F. N., The extracellular portion of the human blood-air barrier and its relation to tissue space, *Anat. Rec.*, 1961, **139**, 105.
8. Weibel, E. R., Morphometry of the Human Lung, Berlin-Göttingen-Heidelberg, Springer, and New York, Academic Press, Inc., 1963.
9. Riley, R. L., Cournand, A., and Donald, K. W., Analysis of factors affecting partial pressures of O_2 and CO_2 in gas and blood of lungs: Theory; Methods, *J. Appl. Physiol.*, 1951, **4**, 77; 102.
10. Forster, R. E., Exchange of gases between alveolar air and pulmonary capillary blood: pul-

monary diffusing capacity, *Physiol. Rev.*, 1957, **37**, 391.

11. MEESSEN, H., Die Pathomorphologie der Diffusion und Perfusion, *Verhandl. deutsch. path. Ges.*, 1960, **44**, 98.
12. FRITTS, H. W., STRAUSS, B., and WICHERN, W., JR., Utilization of oxygen in the lungs of patients with diffuse, non-obstructive pulmonary disease, *Tr. Am. Assn. Phys.*, 1963, in press.
13. WEIBEL, E. R., and GOMEZ, D. M., Architecture of the human lung, *Science*, 1962, **137**, 577.
14. WEIBEL, E. R., Morphometrische Bestimmung von Zahl, Volumen und Oberfläche der Alveolen und Kapillaren der menschlichen Lunge, *Z. Zellforsch.*, 1962, **57**, 648.
15. CHALKLEY, H. W., CORNFIELD, J., and PARK, H., A method for estimating volume surface ratios, *Science*, 1949, **110**, 295.
16. WEIBEL, E. R., Principles and methods for the morphometric study of the lung and other organs, *Lab. Inv.*, 1963, **12**, 131.
17. HENNING, A., Das Problem der Kernmessung. Eine Zusammenfassung und Erweiterung der mikroskopischen Messtechnik, *Mikroskopie*, 1957, **12**, 174.
18. SABATINI, D. D., BENSCH, K., and BARRNETT, R. J., Cytochemistry and electron microscopy. The preservation of cellular ultrastructure and enzymatic activity by aldehyde fixation, *J. Cell Biol.*, 1963, **17**, 19.
19. LUFT, J. H., Improvements in epoxy resin embedding methods, *J. Biophysic. and Biochem. Cytol.*, 1961, **9**, 409.
20. KARNOVSKY, M. J., Simple methods for "staining with lead" at high pH in electron microscopy, *J. Biophysic. and Biochem. Cytol.*, 1961, **11**, 729.